

AMMRC TR 78-15

AD A058573

6^{new}
LEVEL II

**STRESS INTENSITY ESTIMATES FOR A
PERIPHERALLY CRACKED
SPHERICAL VOID AND A
HEMISPHERICAL SURFACE PIT**

FRANCIS I. BARATTA
MECHANICS OF MATERIALS DIVISION

DDC
PREPARED
SEP 14 1978
F

AD No. _____
DDC FILE COPY

March 1978

Approved for public release; distribution unlimited.

ARMY MATERIALS AND MECHANICS RESEARCH CENTER
Watertown, Massachusetts 02172

78 09 01 062

The findings in this report are not to be construed as an official Department of the Army position, unless so designated by other authorized documents.

Mention of any trade names or manufacturers in this report shall not be construed as advertising nor as an official indorsement or approval of such products or companies by the United States Government.

DISPOSITION INSTRUCTIONS

Destroy this report when it is no longer needed.
Do not return it to the originator.

UNCLASSIFIED

SECURITY CLASSIFICATION OF THIS PAGE (When Data Entered)

REPORT DOCUMENTATION PAGE		READ INSTRUCTIONS BEFORE COMPLETING FORM
1. REPORT NUMBER AMMRG-TR-78-15	2. GOVT ACCESSION NO.	3. RECIPIENT'S CATALOG NUMBER
4. TITLE (and Subtitle) STRESS INTENSITY ESTIMATES FOR A PERIPHERALLY CRACKED SPHERICAL VOID AND A HEMISPHERICAL SURFACE PIT		5. TYPE OF REPORT & PERIOD COVERED Final Report, PERFORMING ORG. REPORT NUMBER
6. AUTHOR(s) Francis I. Baratta		8. CONTRACT OR GRANT NUMBER(s)
9. PERFORMING ORGANIZATION NAME AND ADDRESS Army Materials and Mechanics Research Center Watertown, Massachusetts 02172 DRXMR-TM		10. PROGRAM ELEMENT, PROJECT, TASK AREA & WORK UNIT NUMBERS D/A Project: 1L162105AH84 AMCMS Code: 612105.H840011 Agency Accession:
11. CONTROLLING OFFICE NAME AND ADDRESS U. S. Army Materiel Development and Readiness Command, Alexandria, Virginia 22333		12. REPORT DATE March 1978
14. MONITORING AGENCY NAME & ADDRESS (if different from Controlling Office)		13. NUMBER OF PAGES 9
		15. SECURITY CLASS. (of this report) Unclassified 15a. DECLASSIFICATION/DOWNGRADING SCHEDULE
16. DISTRIBUTION STATEMENT (of this Report) Approved for public release; distribution unlimited. (12) 15 p		
17. DISTRIBUTION STATEMENT (of the abstract entered in Block 20, if different from Report)		
18. SUPPLEMENTARY NOTES To be published in the Journal of the American Ceramic Society.		
19. KEY WORDS (Continue on reverse side if necessary and identify by block number) Ceramic materials Voids Stress intensity Surface pits		
20. ABSTRACT (Continue on reverse side if necessary and identify by block number) (SEE REVERSE SIDE)		

DD FORM 1 JAN 73 1473

EDITION OF 1 NOV 65 IS OBSOLETE

UNCLASSIFIED

SECURITY CLASSIFICATION OF THIS PAGE (When Data Entered)

403 105

UNCLASSIFIED

SECURITY CLASSIFICATION OF THIS PAGE(When Data Entered)

Block No. 20

ABSTRACT

Stress intensity factors are estimated for three-dimensional defects which occur in ceramic bodies. The two idealized cases considered are: (A) a spherical void with a circumferential crack at its equator stressed by uniaxial tension at infinity, and (B) a hemispherical pit at a free surface of a semi-infinite body also stressed by uniaxial tension with a circumferential crack at the semiequator of the pit. These stress intensity factors, which are given as a function of the crack length L to radius R of the spherical void or hemispherical pit, are considered as estimates because of the approximate nature of the analysis.

ACCESSION for	
NTIS	White Section <input checked="" type="checkbox"/>
DDC	Buff Section <input type="checkbox"/>
UNANNOUNCED	
JUSTIFICATION	
BY	
DISTRIBUTION/AVAILABILITY CODES	
Dist	or SPECIAL
A	

UNCLASSIFIED

SECURITY CLASSIFICATION OF THIS PAGE(When Data Entered)

INTRODUCTION

Researchers in recent years, such as Evans and Tappin,¹ Molner and Rice,² Baratta et al.,³ and Bansal and Duckworth,⁴ to name a few, have attempted to utilize linear elastic fracture mechanics to determine fracture energy or mode I fracture toughness (K_{IC}) of ceramic materials from individual tension or bend specimens by strength and flaw characterization. This attractive approach, if accurately accomplished, is worthwhile pursuing because it will provide in situ K_{IC} data from a simple specimen configuration. However, it is difficult to accurately assess stress intensity factors associated with even regularly-shaped single inherent flaws in ceramic materials because of the complexity of three-dimensional mathematical analyses. Only a limited number of such solutions are available. Although there are other reasons why stress intensity factors associated with inherent flaws in materials are ill defined, such as irregular shape, defects distribution, etc., only those single flaws of regular shape which do occur⁴ in ceramic materials, see Kirchner et al.⁵ also, are considered here. Such results, although approximate, and heretofore unavailable, will aid in fracture mechanics applications and provide guidance until more rigorous analyses become available.

Therefore, the object of this paper is to estimate stress intensity factors for (a) a spherical void with a circumferential crack at its equator in an infinite body under uniaxial tensile stress, as shown in Figure 1, and also include

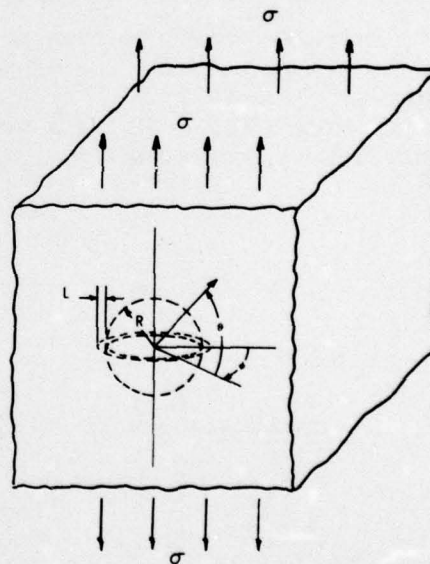


Figure 1. A spherical void with a circumferential crack at its equator.

1. EVANS, A. G., and TAPPIN, G. *The Effects of Microstructure on the Stress to Propagate Inherent Flaws*. Proc. Br. Ceram. Soc., no. 20, 1972, p. 275-297.
2. MOLNER, B. K., and RICE, R. W. *Strength Anisotropy in Lead Zirconate Titanate Transducer Rings*. Am. Ceram. Soc. Bul., v. 52, no. 6, 1973, p. 505-509.
3. BARATTA, F. I., DRISCOLL, G. W., and KATZ, R. N. *The Use of Fracture Mechanics and Fractography to Define Surface Finish Requirements for Si_3N_4 in Ceramics for High Performance Applications*. J. J. Burke, A. E. Gorum, and R. N. Katz, eds., Brook Hill, Chestnut Hill, Massachusetts, 1974.
4. BANSAL, K., and DUCKWORTH, W. H. *Fracture Stress as Related to Flaw and Fracture Mirror Sizes*. J. Am. Ceram. Soc., v. 6, nos. 7-8, 1977, p. 304-310.
5. KIRCHNER, H. P., GROVER, R. M., and SOTTER, W. A. *Characteristics of Flaws at Fracture Origins and Fracture Stress-Flaw Size Relations in Various Ceramics*. Mtls. Sci. and Eng., no. 22, 1976, p. 147-156.

78 09 01 062

(b) a circumferentially-cracked hemispherical pit at a free surface of a semi-infinite body also stressed by uniaxial tension, as shown in Figure 2. Stress intensity estimates for these two cases will be developed.

PROCEDURE

The procedure is one of applying the appropriate stress, compatible with the defect discontinuity, to the crack tip for the known limiting cases of stress intensity and utilizing an interpolation scheme between limits to determine intermediate values. According to Barenblatt,⁶ the stress intensity can be obtained by loading the crack faces with the negative of the stresses that would normally exist on the plane of the crack, if the crack was absent. However, in the analyses to follow, rather than apply the stress distribution to the crack face, only the stress caused by the defect discontinuity will be applied to the crack tip as suggested by Cartwright.*

In order to demonstrate the details of the procedure and evaluate the validity of the approach, it will be applied to a problem already solved by more accurate means. Consider a crack in a region of high stress concentration, such as a single radial crack originating from a circular hole in an infinite plate subjected to uniaxial uniform tension at infinity, as shown in Figure 3a. This problem has been successfully solved by Bowie⁷ and will be used to evaluate the following approach.

We initially consider the crack length L to be very small compared to the hole radius R . Since the hole radius is very large compared to the crack length we can consider it to be at an edge of a semi-infinite plate, as shown by the equivalent system in Figure 3b, but with a stress distribution $\sigma_\theta(r)$ that arises because of the hole. The normalized stress intensity ratio $K_I/\sigma\sqrt{\pi L}$ for an edge crack in a

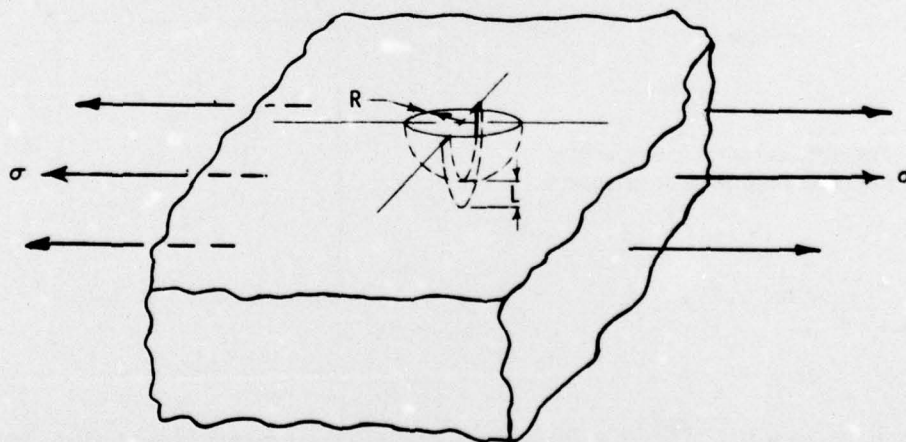


Figure 2. A hemispherical surface pit with a circumferential crack at its semiequator.

*CARTWRIGHT, D. J., University of Southampton, England, Internal Publication.

6. BARENBLATT, G. I. *The Mathematical Theory of Equilibrium Cracks in Brittle Fracture*. Advances in Applied Mechanics, v. 7, Academic Press, 1962.

7. BOWIE, O. L. *Analysis of an Infinite Plate Containing Radial Cracks Originating at the Boundary of an Internal Circular Hole*. J. Math. Phys., v. 35, no. 11, 1956, p. 60-71.

semi-infinite plate stressed in tension at infinity given by Paris and Sih⁸ is $K_I/\sigma\sqrt{\pi L} = 1.12$, where σ is the remotely applied uniform tensile stress. At the opposite extreme when the crack length is very large compared to the hole radius, i.e., $L/R \rightarrow \infty$, the normalized stress intensity ratio $K_I/\sigma\sqrt{\pi L} = 0.707$, from Reference 7. It appears that this ratio is dependent upon some function of L/R which has limits of 1.12 when $L/R = 0$ and 0.707 when $L/R \rightarrow \infty$. Thus, intermediate values of the normalized stress intensity ratio can be approximated by choosing a function which is well behaved between the above stated limits. The function arbitrarily chosen for this problem as well as those to follow is of the form:

$$f(L/R) = c - k(\tan^{-1} L/R)^m. \quad (1)$$

Thus, for a circular hole with one radial crack the normalized stress intensity ratio is:

$$K_I/\sigma_\theta(r)\sqrt{\pi L} = f(L/R) = c - k(\tan^{-1} L/R)^m, \quad (2)$$

where $\sigma_\theta(r)$ is the stress distribution caused by the circular hole, provided by Timoshenko and Goodier,⁹ which is

$$\sigma_\theta(r) = \sigma[1 + (1/2)(R/r)^2 + (3/2)(R/r)^4], \quad r \geq R, \quad (3)$$

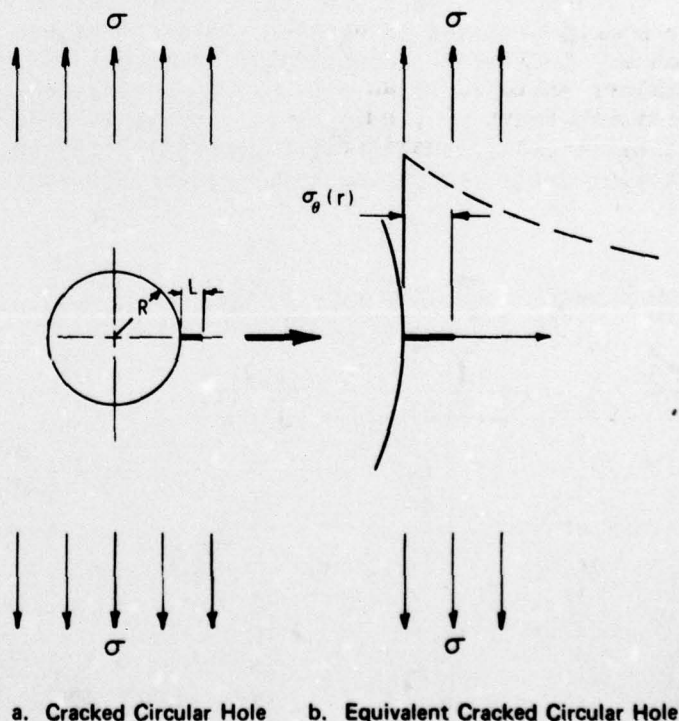


Figure 3. Circular hole with a single radial crack.

8. PARIS, P. C., and SIH, G. C. *Stress Analysis of Cracks*. ASTM-STP 381, 1970, p. 30-83.

9. TIMOSHENKO, S., and GOODIER, J. N. *Theory of Elasticity*. McGraw-Hill Book Company, Inc., 2nd Ed., 1951.

where r is the radial distance from the center of the hole. Substitution of Equation 3 into Equation 2 and transforming the coordinate axis r by $R + L$, gives:

$$K_I/\sigma\sqrt{\pi L} = [c - k(\tan^{-1} L/R)^m] [1 + (1/2)\left(\frac{1}{L/R + 1}\right)^2 + (3/2)\left(\frac{1}{L/R + 1}\right)^4]. \quad (4)$$

Equation 4 represents the estimated normalized stress intensity ratio $K_I/\sigma\sqrt{\pi L}$ for a radial crack of length L emanating from a circular hole of radius R . The particular constants which appear in Equation 4 are readily determined by knowing $c = 1.12$ when $L/R = 0$; k and m are found by allowing $f(L/R) = 0.707$ when $L/R = \infty$, and $f(L/R) = 0.94$ when $L/R = 3.0$ (taken from Reference 7). The latter value was chosen so that the error span on the function would be minimized throughout the total range of L/R . Thus, $c = 1.12$; k was found to be 0.119 and m to be 2.748.

Equation 4 was then utilized to obtain $K/\sigma\sqrt{\pi L}$ as a function of L/R from 0 to infinity. It is seen that these results shown in Table 1 are within $\pm 6\%$ when compared to the more accurate data of Reference 8. Although the results of this procedure are approximate, it is believed that the errors involved when applied to the problems represented by Figures 1 and 2 will be of similar magnitude as those given in Table 1. Thus, a similar approach is used to solve these problems of interest.

Peripherally-Cracked Spherical Void

Goodier¹⁰ provides the stress distribution for a spherical defect in an infinite medium stressed in tension. Because of the defect three stresses are developed, which are indicated schematically in Figure 4; they are a radial stress σ_r acting normal to the interface; a stress σ_θ acting in a tangential direction to a meridian (the north-south pole axis of the sphere is considered aligned with the axis of the applied stress); and another tangential stress σ_ϕ normal to both σ_r and σ_θ . In the following analysis, the maximum tensile stress is assumed to cause crack initiation.

Table 1. COMPARISON OF APPROXIMATE TO EXACT STRESS INTENSITY RESULTS FOR A CIRCULAR HOLE WITH A RADIAL CRACK

L/R	$K_I/\sigma\sqrt{\pi L}$		
	From Eq. 3	Reference 7	% Difference
0	3.36	3.39	-1
0.1	2.73	2.73	0
0.2	2.32	2.30	+1
0.3	2.04	2.04	0
0.4	1.83	1.86	-2
0.5	1.69	1.73	-2
0.6	1.56	1.64	-5
0.8	1.40	1.47	-5
1.0	1.29	1.37	-6
1.5	1.13	1.18	-4
2.0	1.03	1.06	-3
3.0	0.94	0.94	0
5.0	0.86	0.81	+6
10.0	0.78	0.75	+4
∞	0.708	0.707	0

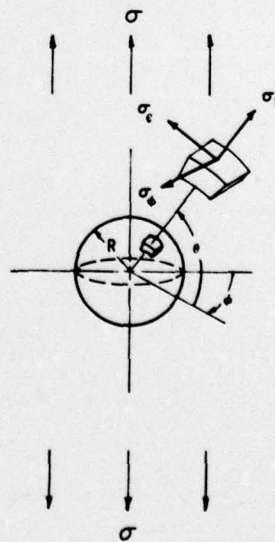


Figure 4. Coordinate system to describe the stress state around a spherical void.

10. GOODIER, J. N. *Concentration of Stress Around Spherical and Cylindrical Inclusions and Flaws*. Trans. Am. Soc. M. E., v. 55, 1933, p. 39-44.

It is indicated in Reference 10 that the maximum tensile stress for a spherical void occurs when $\theta = 0$, resulting in a "hoop stress" σ_θ , which girdles the equator. It is expected that this tensile stress, if becoming large enough, can initiate an axisymmetric crack and extend it in the radial direction as envisioned in Figure 1. The stress distribution when $\theta = 0$ from Reference 10 is given in the following equation:

$$\sigma_\theta(r) = \sigma \left(\frac{1}{2(7-5\nu)} [(4-5\nu)(R/r)^3 + 9(R/r)^5] + 1 \right), \quad (5)$$

where ν is Poisson's ratio of the material and r is the radial distance from the center of the spherical void ($r \geq R$).

To obtain an approximation for the stress intensity factor associated with Figure 1, we again initially assume that the crack length L is small compared to the sphere radius R . Also, as before, we further assume that when the crack is small, the influence of the spherical void on the crack is negligible and thus can be considered as an edge crack as shown in Figure 3b, but with a stress distribution $\sigma_\theta(r)$ provided by Equation 5 that arises because of the spherical void. Also, we shall assume that Equation 1 is applicable as well as the constants (except k) previously given as $c = 1.12$ and $m = 2.748$; k is determined by realizing that in the extreme limit when $L/R \rightarrow \infty$ the defect geometry approaches a disk crack and thus $K_I/\sigma\sqrt{\pi L} \rightarrow 2/\pi$, according to Sneddon.¹¹ Therefore, making use of this end limit in Equation 1, which is substituted along with Equation 5 into Equation 2, results in the following normalized stress intensity expression:

$$K_I/\sigma\sqrt{\pi L} = [c - k(\tan^{-1} L/R)^m] \left(\frac{1}{2(7-5\nu)} \left[(4-5\nu) \left(\frac{1}{L/R+1} \right)^3 + 9 \left(\frac{1}{L/R+1} \right)^5 \right] + 1 \right), \quad (6)$$

where $c = 1.12$, $m = 2.748$, and k is determined to be 0.101.

The resulting calculations using Equation 6, which represents the normalized stress intensity ratio for a spherical void cracked at its equator and stressed by uniform uniaxial tension at infinity, are shown in Table 2 as a function of L/R from 0 to infinity and for $\nu = 0.25$ and 0.30.

Peripherally-Cracked Hemispherical Pit

The final case considered is a hemispherical pit at a free surface of a semi-infinite body with a crack initiated at the semiequator of the pit and extended radially by a uniaxial uniform tensile stress as shown in Figure 2. As outlined previously, we initially assume that L is very small compared to R . We further assume that when the crack is small, the influence of the hemispherical pit on the crack is negligible and thus can be considered as an edge crack as shown in

Table 2. STRESS INTENSITY RATIO FOR A PERIPHERALLY-CRACKED SPHERICAL VOID

L/R	$K_I/\sigma\sqrt{\pi L}$	
	0.25	0.30
0	2.26	2.30
0.15	1.73	1.75
0.35	1.41	1.41
0.55	1.26	1.26
1.00	1.10	1.08
2.00	0.94	0.93
3.00	0.86	0.86
5.00	0.79	0.79
10.00	0.72	0.72
∞	0.64	0.64

11. SNEDDON, I. N. *The Distribution of Stress in the Neighborhood of a Crack in an Elastic Solid*. Proc. Roy. Soc. London, v. A-187, 1946.

Figure 3b, with the stress distribution $\sigma_\theta(r)$ that arises because of the surface pit discontinuity. Again, as before, we utilize Equation 2, with $c = 1.12$ and $m = 2.748$; but determine k from the end limit when $L/R \rightarrow \infty$. Smith and Alavi¹² give the variation of $K_I/\sigma\sqrt{\pi L}$ around the semicircular crack boundary and indicate that the maximum value occurs at the junction of the crack with the free surface and is $1.21 \times 2/\pi$. This results in $k = 0.140$.

The stress distribution $\sigma_\theta(r)$ is provided by Eubanks,¹³ who has determined the variation of the circumferential stress along the axis of symmetry as a function of r at the base of the pit. Equation 2, including the constants previously given, i.e., $c = 1.12$, $m = 2.748$, and $k = 0.140$, and the normalized stress distribution¹³ $\sigma_\theta(r)/\sigma$ given in tabular form will provide the normalized stress intensity ratio for a peripherally-cracked hemispherical surface pit with $\nu = 0.25$. Such results, including $\sigma_\theta(r)/\sigma$, are given in Table 3 as a function of L/R from 0 to infinity.

RESULTS AND DISCUSSION

The results of the procedure applied to the known stress intensity case of one radial crack emanating from a circular hole indicated that the error was $\pm 6\%$. The procedure was then extended to the two cases of interest assuming that engineering accuracy would be preserved.

Table 2 presents the normalized stress intensity ratio $K_I/\sigma\sqrt{\pi L}$ as a function of L/R from 0 to infinity for the circumferentially-cracked spherical void, with Poisson's ratio being 0.25 and 0.30. This table indicates that Poisson's ratio, within the range considered, has little effect on the stress intensity ratio.

Table 3 presents $K_I/\sigma\sqrt{\pi L}$ as a function of L/R from 0 to infinity for the circumferentially-cracked hemispherical surface pit when $\nu = 0.25$. It is evident that the magnitude of the normalized stress intensity ratio for the peripherally-cracked surface pit is greater than that of the peripherally-cracked spherical void for the same given L/R value.

Restrictions on Application

The application of Equation 6 and Tables 2 and 3 has certain restrictions resulting from the implied assumptions given in References 10 and 13 when determining the appropriate stress distributions. These restrictions are:

- the material is isotropic and homogeneous;
- the defect is very large compared to the grain size of the crystalline aggregate;

Table 3. NORMALIZED STRESS INTENSITY RATIO FOR A PERIPHERALLY-CRACKED HEMISPHERICAL SURFACE PIT, WITH $\nu = 0.25$

L/R	$\sigma_\theta(r)/\sigma$	$K_I/\sigma\sqrt{\pi L}$
0	2.23	2.50
0.15	1.63	1.82
0.35	1.29	1.44
0.55	1.15	1.27
1.00	1.04	1.11
2.00	1.00	0.99
3.00	1.00	0.93
5.00	1.00	0.88
10.00	1.00	0.83
∞	1.00	0.77

- SMITH, F. W., and ALAVI, M. J. *Stress Intensity Factors for a Part-Through Circular Surface Flaw*. Proc. 1st Intl. Conf. on Pressure Vessel Tech., Delft, Holland, 1969.
- EUBANKS, R. A. *Stress Concentration Due to a Hemispherical Pit at a Free Surface*. J. Appl. Mech., v. 21, 1954, p. 57-62.

- c. there are no other defects closer than four diameters away;
- d. the cracked spherical void can be no closer than four diameters to the body boundary; and
- e. the cracked hemispherical pit on the free surface can be no closer than four diameters away from any other body boundary.

SUMMARY

1. An approximate method is presented which allows estimates of normalized stress intensity for three-dimensional defects such as a circumferentially-cracked spherical void and a circumferentially-cracked hemispherical surface pit as a function of crack length to void or pit radius when L/R is between 0 and infinity.
2. The three-dimensional defects considered in this paper can be thought of as being two-dimensional at their limits when $L/R = 0$ and when $L/R \rightarrow \text{infinity}$. With the appropriately known limiting normalized stress intensity values obtained from the literature, an interpolation scheme was employed to obtain intermediate values when L/R was between 0 and infinity. The results given by Equation 6 and Tables 2 and 3 are expected to be within engineering accuracy.
3. It was shown that for the spherical void case the variation of Poisson's ratio between 0.25 and 0.30 had little effect on stress intensity.
4. It was also shown that the stress intensity factor associated with a circumferentially-cracked hemispherical surface pit was greater than that of a circumferentially-cracked spherical void for the same given L/R value.
5. The restrictions indicated in the previous section must be recognized when applying Equation 6 or utilizing Tables 2 and 3.

ACKNOWLEDGMENT

The author wishes to acknowledge the helpful advice given by David J. Cartwright from the University of Southampton, England, NATO Fellow to the Army Materials and Mechanics Research Center.

DISTRIBUTION LIST

No. of Copies	To	No. of Copies	To
1	Office of the Director, Defense Research and Engineering, The Pentagon, Washington, D. C. 20301		Commander, U. S. Army Armament Research and Development Command, Aberdeen Proving Ground, Maryland 21010
12	Commander, Defense Documentation Center, Cameron Station, Building 5, 5010 Duke Street, Alexandria, Virginia 22314	1	ATTN: DRDAR-QAC-E
1	Metals and Ceramics Information Center, Battelle Columbus Laboratories, 505 King Avenue, Columbus, Ohio 43201		Chief, Benet Weapons Laboratory, LCWSL, USA ARRADCOM, Watervliet Arsenal, Watervliet, New York 12189
	Office of the Deputy Chief of Staff for Research, Development, and Acquisition, Washington, D. C. Washington, D. C. 20310	1	ATTN: DRDAR-LCB-TL
2	ATTN: DAMA-ARZ		Director, Eustis Directorate, U. S. Army Air Mobility Research and Development Laboratory, Fort Eustis, Virginia 23604
	Commander, Army Research Office, P. O. Box 12211, Research Triangle Park, North Carolina 27709	1	ATTN: Mr. J. Robinson, DAVDL-E-MOS (AVRADCOM)
1	ATTN: Information Processing Office		U. S. Army Aviation Training Library, Fort Rucker, Alabama 36360
1	Dr. F. W. Schmiedeshoff	1	ATTN: Buildings 5906-5907
	Commander, U. S. Army Materiel Development and Readiness Command, 5001 Eisenhower Avenue, Alexandria, Virginia 22333		Commander, U. S. Army Agency for Aviation Safety, Fort Rucker, Alabama 36362
1	ATTN: DRCLDC, Mr. R. Zentner	1	ATTN: Librarian, Building 4905
	Commander, U. S. Army Communications Research and Development Command, Fort Monmouth, New Jersey 07703		Commander, USACDC Air Defense Agency, Fort Bliss, Texas 79916
1	ATTN: DRDCO-GG-TD	1	ATTN: Technical Library
1	DRDCO-GG-DM		Commander, U. S. Army Engineer School, Fort Belvoir, Virginia 22060
	Commander, U. S. Army Missile Research and Development Command, Redstone Arsenal, Alabama 35809	1	ATTN: Library
1	ATTN: DRDMI-RKK, Mr. C. Martens, Bldg. 7120		Commander, U. S. Army Engineer Waterways Experiment Station, Vicksburg, Mississippi 39180
	Commander, U. S. Army Armament Research and Development Command, Dover, New Jersey 07801	1	ATTN: Research Center Library
2	ATTN: Technical Library		Commander, U. S. Army Mobility Equipment Research and Development Center, Fort Belvoir, Virginia 22060
1	DRDAR-SCM, Mr. J. D. Corrie	1	ATTN: DRDME-MW, Dr. J. W. Bond
1	Dr. J. Fraiser		Commander, Naval Air Engineering Center, Lakehurst, New Jersey 08733
	Commander, U. S. Army Natick Research and Development Command, Natick, Massachusetts 01760	1	ATTN: Technical Library, Code 1115
1	ATTN: Technical Library		Director, Structural Mechanics Research, Office of Naval Research, 800 North Quincy Street, Arlington, Virginia 22203
1	Dr. E. W. Ross	1	ATTN: Dr. N. Perrone
1	DRDNA, Dr. L. A. McClaine		Naval Air Development Center, Aero Materials Department, Warminster, Pennsylvania 18974
	Commander, U. S. Army Satellite Communications Agency, Fort Monmouth, New Jersey 07703	1	ATTN: J. Viglione
1	ATTN: Technical Document Center		David Taylor Naval Ship Research and Development Laboratory, Annapolis, Maryland 21402
	Commander, U. S. Army Tank-Automotive Research and Development Command, Warren, Michigan 48090	1	ATTN: Dr. H. P. Chu
1	ATTN: DRDTA-RKA		Naval Research Laboratory, Washington, D. C. 20375
1	DRDTA-UL, Technical Library	1	ATTN: C. D. Beachem, Head, Adv. Mat'l's
	Commander, White Sands Missile Range, New Mexico 88002	1	Tech Br. (Code 6310)
1	ATTN: STEWS-WS-VT	1	Dr. J. M. Krafft - Code 8430
	Commander, Aberdeen Proving Ground, Maryland 21005	1	E. A. Lange
1	ATTN: STEAP-TL, Bldg. 305	1	Dr. P. P. Puzak
	Commander, Frankford Arsenal, Philadelphia, Pennsylvania 19137	1	R. J. Sanford - Code 8436
1	ATTN: Library, H1300, Bl. 51-2	1	A. M. Sullivan
	Commander, U. S. Army Ballistic Research Laboratory, Aberdeen Proving Ground, Maryland 21005	1	R. W. Rice
1	ATTN: Dr. R. Vitali	1	S. W. Freiman
1	Dr. G. L. Filbey		Chief of Naval Research, Arlington, Virginia 22217
1	Dr. W. Gillich	1	ATTN: Code 471
	Commander, Harry Diamond Laboratories, 2800 Powder Mill Road, Adelphi, Maryland 20783		Naval Weapons Laboratory, Washington, D. C. 20390
1	ATTN: Technical Information Office	1	ATTN: H. W. Romine, Mail Stop 103
	Commander, Picatinny Arsenal, Dover, New Jersey 07801	1	Ship Research Committee, Maritime Transportation Research Board, National Research Council, 2101 Constitution Ave., N. W., Washington, D. C. 20418
1	ATTN: Mr. J. Pearson		Air Force Materials Laboratory, Wright-Patterson Air Force Base, Ohio 45433
1	G. Randers-Pehrson	2	ATTN: AFML/MXE/E. Morrissey
1	Mr. A. Garcia	1	AFML/LC
1	SARPA-RT-S	1	AFML/LLP/D. M. Forney, Jr.
	Commander, Redstone Scientific Information Center, U. S. Army Missile Research and Development Command, Redstone Arsenal, Alabama 35809	1	AFML/MSC/Stanley Schulman
1	ATTN: DRDMI-TB	1	AFML/LNC/T. J. Reinhart
	Commander, Watervliet Arsenal, Watervliet, New York 12189		Air Force Flight Dynamics Laboratory, Wright-Patterson Air Force Base, Ohio 45433
1	ATTN: Dr. T. Davidson	1	ATTN: AFFDL (FBS), C. Wallace
1	Mr. D. P. Kendall	1	AFFDL (FBE), G. D. Sendeckyj
1	Mr. J. F. Throop	1	AFFDL (FB), Dr. J. C. Halpin
	Commander, U. S. Army Foreign Science and Technology Center, 220 7th Street, N. E., Charlottesville, Virginia 22901		National Aeronautics and Space Administration, Washington, D. C. 20546
1	ATTN: Mr. Marley, Military Tech	1	ATTN: Mr. B. G. Achhammer
		1	Mr. G. C. Deutsch - Code RW
			National Aeronautics and Space Administration, Marshall Space Flight Center, Huntsville, Alabama 35812
		1	ATTN: R. J. Schwinghamer, EH41, Director, M&P Laboratory
		1	Mr. W. A. Wilson, EH41, Building 4612

No. of Copies	To
1	National Aeronautics and Space Administration, Langley Research Center, Hampton, Virginia 23665
1	ATTN: Mr. H. F. Hardrath, Mail Stop 188M
1	Mr. R. Foye, Mail Stop 188A
1	National Aeronautics and Space Administration, Lewis Research Center, 21000 Brookpark Road, Cleveland, Ohio 44135
1	ATTN: Mr. S. S. Manson
1	Dr. J. E. Srawley, Mail Stop 105-1
1	Mr. W. F. Brown, Jr.
1	Mr. M. H. Hirschberg, Head, Fatigue Research Section, Mail Stop 49-1
1	Mechanical Properties Data Center, Belfour Stulen, Inc., 13917 W. Bay Shore Drive, Traverse City, Michigan 49684
1	National Bureau of Standards, U. S. Department of Commerce, Washington, D. C. 20234
1	ATTN: Mr. J. A. Bennett
1	Mr. W. F. Anderson, Atomics International, Canoga Park, California 91303
1	Midwest Research Institute, 425 Coker Boulevard, Kansas City, Missouri 64110
1	ATTN: Mr. G. Gross
1	Mr. A. Hurlich, Convair Div., General Dynamics Corp., Mail Zone 630-01, P. O. Box 80847, San Diego, California 92138
1	Mr. J. G. Kaufman, Alcoa Research Laboratories, New Kensington, Pennsylvania 15068
1	Mr. P. N. Randall, TRW Systems Group - 0-1/2210, One Space Park, Redondo Beach, California 90278
1	Dr. E. A. Steigerwald, TRW Metals Division, P. O. Box 250, Minerva, Ohio 44657
1	Dr. George R. Irwin, Department of Mechanical Engineering, University of Maryland, College Park, Maryland 20742
1	Mr. W. A. Van der Sluys, Research Center, Babcock and Wilcox, Alliance, Ohio 44601
1	Mr. B. M. Wundt, 2346 Shirl Lane, Schenectady, New York 12309
1	Battelle Columbus Laboratories, 505 King Avenue, Columbus, Ohio 43201
1	ATTN: Mr. J. Campbell
1	Dr. G. T. Hahn
1	R. G. Hoagland, Metal Science Group
1	Dr. E. Rybicki
1	General Electric Company, Schenectady, New York 12010
1	ATTN: Mr. A. J. Brothers, Materials and Processes Laboratory
1	General Electric Company, Schenectady, New York 12309
1	ATTN: Mr. H. F. Bueckner, Large Steam Turbine Generator Department
1	Mr. S. Yukawa, Metallurgy Unit
1	Mr. E. E. Zwicky, Jr.
1	General Electric Company, Knolls Atomic Power Laboratory, P. O. Box 1072, Schenectady, New York 12301
1	ATTN: Mr. F. J. Mehringer
1	Dr. L. F. Coffin, Room 1C41-K1, Corp. R&D, General Electric Company, P. O. Box 8, Schenectady, New York 12301
1	United States Steel Corporation, Monroeville, Pennsylvania 15146
1	ATTN: Mr. S. R. Novak
1	Dr. A. K. Shoemaker, Research Laboratory, Mail Stop 78
1	Westinghouse Electric Company, Bettis Atomic Power Laboratory, P. O. Box 109, West Mifflin, Pennsylvania 15122
1	ATTN: Mr. M. L. Parrish
1	Westinghouse Research and Development Center, 1310 Beulah Road, Pittsburgh, Pennsylvania 15235
1	ATTN: Mr. E. T. Wessel
1	Mr. M. J. Manjoine
1	Dr. Alan S. Tetelman, Failure Analysis Associates, Suite 4, 11777 Mississippi Avenue, Los Angeles, California 90025

No. of Copies	To
1	Brown University, Providence, Rhode Island 02912
1	ATTN: Prof. J. R. Rice
1	Prof. W. N. Findley, Division of Eng., Box D
1	Prof. P. C. Paris
1	Carnegie-Mellon University, Department of Mechanical Engineering, Schenley Park, Pittsburgh, Pennsylvania 15213
1	ATTN: Dr. J. L. Swedlow
1	Prof. J. D. Lubahn, Colorado School of Mines, Golden, Colorado 80401
1	Prof. J. Dvorak, Civil Engineering Department, Duke University, Durham, North Carolina 27706
1	George Washington University, School of Engineering and Applied Sciences, Washington, D. C. 20052
1	ATTN: Dr. H. Liebowitz
1	Lehigh University, Bethlehem, Pennsylvania 18015
1	ATTN: Prof. G. C. Sih
1	Prof. R. Roberts
1	Prof. R. P. Wei
1	Prof. F. Erodgan
1	Massachusetts Institute of Technology, Cambridge, Massachusetts 02139
1	ATTN: Prof. B. L. Averbach, Materials Center, 13-5082
1	Prof. F. A. McClintock, Room 1-304
1	Prof. R. M. Pelloux
1	Prof. T. H. H. Pian, Dept. of Aeronautics and Astronautics
1	Prof. A. S. Argon, Room 1-306
1	Syracuse University, Department of Chemical Engineering and Metallurgy, 409 Link Hall, Syracuse, New York 13210
1	ATTN: Mr. H. W. Liu
1	Dr. V. Weiss, Metallurgical Res. Labs., Bldg. D-6
1	Prof. E. R. Parker, Department of Materials Science and Engineering, University of California, Berkeley, California 94700
1	Prof. W. Goldsmith, Department of Mechanical Engineering, University of California, Berkeley, California 94720
1	University of California, Los Alamos Scientific Laboratory, Los Alamos, New Mexico 87544
1	ATTN: Dr. R. Karp
1	Prof. A. J. McEvily, Metallurgy Department U-136, University of Connecticut, Storrs, Connecticut 06268
1	Prof. D. Drucker, Dean of School of Engineering, University of Illinois, Champaign, Illinois 61820
1	University of Illinois, Urbana, Illinois 61801
1	ATTN: Prof. H. T. Corten, Department of Theoretical and Applied Mechanics, 212 Talbot Lab.
1	Prof. T. J. Dolan, Department of Theoretical and Applied Mechanics
1	Prof. J. Morrow, 321 Talbot Lab.
1	Mr. G. M. Sinclair, Department of Theoretical and Applied Mechanics
1	Prof. R. I. Stephens, Materials Engineering Division, University of Iowa, Iowa City, Iowa 52242
1	Prof. D. K. Felbeck, Department of Mechanical Engineering, University of Michigan, 2046 East Engineering, Ann Arbor, Michigan 48109
1	Dr. M. L. Williams, Dean of Engineering, 240 Benedum Hall, University of Pittsburgh, Pittsburgh, Pennsylvania 15260
1	Prof. A. Kobayashi, Department of Mechanical Engineering, FU-10, University of Washington, Seattle, Washington 98195
1	State University of New York at Stony Brook, Stony Brook, New York 11790
1	ATTN: Prof. Fu-Pen Chiang, Department of Mechanics
1	Director, Army Materials and Mechanics Research Center, Watertown, Massachusetts 02172
2	ATTN: DRXMR-PL
1	DRXMR-AG-MD
1	Author

<p>Army Materials and Mechanics Research Center, Watertown, Massachusetts 02172 STRESS INTENSITY ESTIMATES FOR A PERIPHERALLY CRACKED SPHERICAL VOID AND A HEMISPHERICAL SURFACE PIT - Francis I. Baratta</p> <p>Technical Report AMMRC TR 78-15, March 1978, 9 pp - illus-tables, D/A Project IL162105AH84, AMCMS Code 612105.H840011</p> <p>Stress intensity factors are estimated for three-dimensional defects which occur in ceramic bodies. The two idealized cases considered are (a) a spherical void with a circumferential crack at its equator stressed by uniaxial tension at infinity and (b) a hemispherical pit at a free surface of a semi-infinite body also stressed by uniaxial tension with a circumferential crack at the semiequator of the pit. These stress intensity factors, which are given as a function of the crack length L to radius R of the spherical void or hemispherical pit, are considered as estimates because of the approximate nature of the analysis.</p>	<p>AD</p> <p>UNCLASSIFIED UNLIMITED DISTRIBUTION</p> <p>Key Words Ceramic materials Stress intensity Voids</p>	<p>Army Materials and Mechanics Research Center, Watertown, Massachusetts 02172 STRESS INTENSITY ESTIMATES FOR A PERIPHERALLY CRACKED SPHERICAL VOID AND A HEMISPHERICAL SURFACE PIT - Francis I. Baratta</p> <p>Technical Report AMMRC TR 78-15, March 1978, 9 pp - illus-tables, D/A Project IL162105AH84, AMCMS Code 612105.H840011</p> <p>Stress intensity factors are estimated for three-dimensional defects which occur in ceramic bodies. The two idealized cases considered are (a) a spherical void with a circumferential crack at its equator stressed by uniaxial tension at infinity and (b) a hemispherical pit at a free surface of a semi-infinite body also stressed by uniaxial tension with a circumferential crack at the semiequator of the pit. These stress intensity factors, which are given as a function of the crack length L to radius R of the spherical void or hemispherical pit, are considered as estimates because of the approximate nature of the analysis.</p>	<p>AD</p> <p>UNCLASSIFIED UNLIMITED DISTRIBUTION</p> <p>Key Words Ceramic materials Stress intensity Voids</p>
<p>Army Materials and Mechanics Research Center, Watertown, Massachusetts 02172 STRESS INTENSITY ESTIMATES FOR A PERIPHERALLY CRACKED SPHERICAL VOID AND A HEMISPHERICAL SURFACE PIT - Francis I. Baratta</p> <p>Technical Report AMMRC TR 78-15, March 1978, 9 pp - illus-tables, D/A Project IL162105AH84, AMCMS Code 612105.H840011</p> <p>Stress intensity factors are estimated for three-dimensional defects which occur in ceramic bodies. The two idealized cases considered are (a) a spherical void with a circumferential crack at its equator stressed by uniaxial tension at infinity and (b) a hemispherical pit at a free surface of a semi-infinite body also stressed by uniaxial tension with a circumferential crack at the semiequator of the pit. These stress intensity factors, which are given as a function of the crack length L to radius R of the spherical void or hemispherical pit, are considered as estimates because of the approximate nature of the analysis.</p>	<p>AD</p> <p>UNCLASSIFIED UNLIMITED DISTRIBUTION</p> <p>Key Words Ceramic materials Stress intensity Voids</p>	<p>Army Materials and Mechanics Research Center, Watertown, Massachusetts 02172 STRESS INTENSITY ESTIMATES FOR A PERIPHERALLY CRACKED SPHERICAL VOID AND A HEMISPHERICAL SURFACE PIT - Francis I. Baratta</p> <p>Technical Report AMMRC TR 78-15, March 1978, 9 pp - illus-tables, D/A Project IL162105AH84, AMCMS Code 612105.H840011</p> <p>Stress intensity factors are estimated for three-dimensional defects which occur in ceramic bodies. The two idealized cases considered are (a) a spherical void with a circumferential crack at its equator stressed by uniaxial tension at infinity and (b) a hemispherical pit at a free surface of a semi-infinite body also stressed by uniaxial tension with a circumferential crack at the semiequator of the pit. These stress intensity factors, which are given as a function of the crack length L to radius R of the spherical void or hemispherical pit, are considered as estimates because of the approximate nature of the analysis.</p>	<p>AD</p> <p>UNCLASSIFIED UNLIMITED DISTRIBUTION</p> <p>Key Words Ceramic materials Stress intensity Voids</p>